Nonequilibrium Phase Behavior during the Random Sequential Adsorption of Tethered Hard Disks

Jeffrey J. Gray,[1,*] D. Harley Klein,[1] Roger T. Bonnecaze,[1,2,3,†] and Brian A. Korgel[1,2,3,‡]

[1]*Department of Chemical Engineering, The University of Texas at Austin, Austin, Texas 78712-1062*

[2]*Texas Materials Institute, The University of Texas at Austin, Austin, Texas 78712-1062*

[3]*Center for Nano- and Molecular Science and Technology, The University of Texas at Austin, Austin, Texas 78712-1062*

(Received 10 May 2000)

We simulate random sequential adsorption of tethered hard disks which undergo limited Monte Carlo surface diffusion to study kinetics and nonequilibrium phase behavior. Tethers allow the disks to move within a specified distance of their original adsorption locations, placing a control on the local entropy of each disk. As the surface coverage increases, systems with sufficiently long tethers form hexatic or crystalline lattices, while short tethers frustrate organization. Lattices form with surprisingly short tether lengths — on the order of one disk diameter.

PACS numbers: 05.70.Ln, 64.60.Cn, 68.45.Da, 82.20.Mj

Nonequilibrium systems exhibit markedly different behavior than better understood equilibrium systems. In particular, nonequilibrium systems often exhibit state behavior that is dependent on process history. Here we manipulate a controlling parameter to tune a model nonequilibrium system from a purely kinetic process to a near-equilibrium one.

We present a numerical study of two-dimensional random sequential adsorption (RSA) of *tethered* hard disks. Adsorbed disks diffuse freely on the surface between adsorption attempts, but only within the range of a finite-length tether from the original adsorption location, or anchor point. By varying the tether length from zero to infinity, the adsorption process ranges from pure RSA to a near-equilibrium system. Between these limits, the effects of varied local freedom on disk organization can be studied. Furthermore, this model is appropriate for newly proposed monolayers of tethered nanoparticles, two-dimensional colloidal glasses, or certain systems of adsorbed proteins or cells.

In this study, we observe two new phase transitions in an RSA-type simulation: from liquid to hexatic to crystal, according to the Kosterlitz-Thouless-Halperin-Nelson-Young (KTHNY) scheme for phase transitions in two dimensions [1–3]. The process of sequential adsorption has a significant effect on the phase behavior of this nonequilibrium system. In addition, the phase behavior is coupled to the local entropy of the system as controlled by the disk tether length, L.

We follow the standard RSA procedure where anchors tethered to particles (disks) are added to a random location in a periodically replicated square and overlapping particle placements are rejected [4]. Our cell is $100R \times 100R$, where R is the radius of an adsorbed particle. Between adsorption attempts, particles diffuse according to a Monte Carlo algorithm which selects move magnitudes and directions from two uniform distributions with a maximum step side adjusted every cycle (a cycle is defined as N successful moves, where N is the current number of particles) to obtain 50% acceptance of moves [5]. Diffusion moves that place particles outside of the finite range of the tether as well as those that result in particle-particle overlap are rejected. 200 Monte Carlo cycles are completed after every successful adsorption or after 250 unsuccessful adsorption attempts, so that the dimensionless ratio of diffusion attempts per particle to adsorption attempts is at least the long-time value of 8:5. Since most particle adsorption attempts are unsuccessful (10^{-8} success rate at long times), the rate of surface diffusion far exceeds the rate of particle addition at long times when the important phase behavior is observed.

Kinetic results are shown in Fig. 1 for a range of tether lengths. The tether length does not change the adsorption kinetics at short times (less than one disk placement per equivalent disk area). Soon thereafter, near a fractional surface coverage of 0.35, the kinetic curves diverge, with longer tether-length runs enabling faster and denser

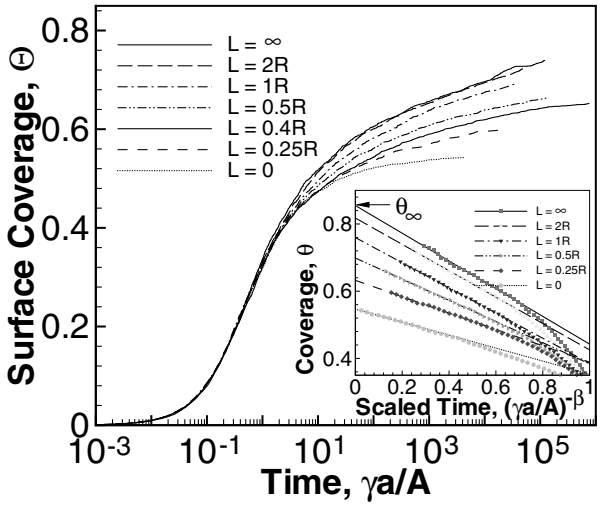

FIG. 1. Kinetic results: Coverage versus time for various tether lengths, L. Inset: Power law extrapolation of kinetic data to the jamming limit, θ_∞.

 0031-9007/00/85(21)/4430(4)$15.00

TABLE I. Kinetic parameters from the power law fit of Eq. (1). Numbers and error estimates are means and standard deviations from the set of curve fits with initial times in $\gamma a/A = \{1, 3, 10, 30, 100\}$.

L/R	θ_∞	α	β
0	0.560 ± 0.004	0.25 ± 0.06	0.45 ± 0.05
0.1	0.58 ± 0.01	0.18 ± 0.04	0.31 ± 0.10
0.25	0.64 ± 0.01	0.25 ± 0.02	0.21 ± 0.07
0.5	0.71 ± 0.01	0.33 ± 0.02	0.18 ± 0.03
1	0.76 ± 0.02	0.36 ± 0.01	0.18 ± 0.05
2	0.85 ± 0.07	0.42 ± 0.03	0.15 ± 0.06
8	0.84 ± 0.04	0.41 ± 0.01	0.15 ± 0.06
∞	0.82 ± 0.03	0.40 ± 0.01	0.16 ± 0.05

adsorption. The inset of Fig. 1 shows the kinetic data replotted in a power law form (generalizing the form observed first by Feder [4] and derived by Swendsen [6]):

$$\theta = \theta_\infty - \alpha(\gamma a/A)^\beta, \tag{1}$$

where θ is the fractional areal coverage on the surface and γ is the number of adsorption attempts normalized by the area of the simulation cell A and the area of a disk a. The jamming limit coverage θ_∞ and the two kinetic parameters α and β are fit to the kinetic data at long times using the Nelder-Mead simplex (direct search) method. Table I summarizes the kinetic results. For classic RSA (i.e., $L/R = 0$), $\beta = 1/2$ theoretically [6]. The fit here of $\beta = 0.45 \pm 0.05$ for a tether length of zero agrees closely. As L increases, the data continue to fit the power law form of Eq. (1), and θ_∞ increases from 0.55 to 0.85. The kinetic coefficient α increases from 0.25 to 0.40, and the kinetic exponent β, often an indicator of the degrees of freedom d in a system ($\beta \sim 1/d$) [6,7], decreases from 0.45 to 0.16. Most of the change in the parameters occurs at surprisingly short tether lengths, on the order of one disk radius. Only a small amount of local freedom dramatically alters the RSA kinetics and θ_∞.

The phase behavior or structural evolution of the system is monitored by direct observation and the statistical measures of the pair distribution function $g(r)$ and the orientational distribution function $g_6(r)$. The orientational distribution function, $g_6(r) = \langle \psi_6^*(0)\psi_6(r)\rangle$, uses the order parameter $\psi_6^{(j)} = \frac{1}{z}\sum_k \exp(6i\theta_{jk})$ evaluated for each particle j, where θ_{jk} is the orientation angle of the line connecting the centers of disk j and each of the z neighboring disks labeled k [8]. Neighbors are defined as all disks closer than $r = 3\sqrt{0.7/\theta}$, which corresponds roughly to the trough between the first and second peak in $g(r)$. The correlation functions are averaged spatially over all particles and also temporally using several sets of diffusion cycles to provide better statistics. Figure 2 shows snapshots of a simulation with tether length $L/R = 5$ at 3 times during its evolution, along with the accompanying plots of $g(r)$ and $g_6(r)$. The structural evolution follows the KTHNY phase scheme [1–3] in that we observe a liquid phase, a hexatic phase, and a crystal phase. The liquid is characterized by disorder and exponentially decaying translational and orientational distribution functions. The hexatic shows a twist along the lattice direction on direct observation (superimposed line in Fig. 2) and exponentially decaying translational order but quasi-long range orientational order as indicated by the algebraic decay of $g_6(r)$. Finally, the crystal has a single box-spanning particle array of constant orientation

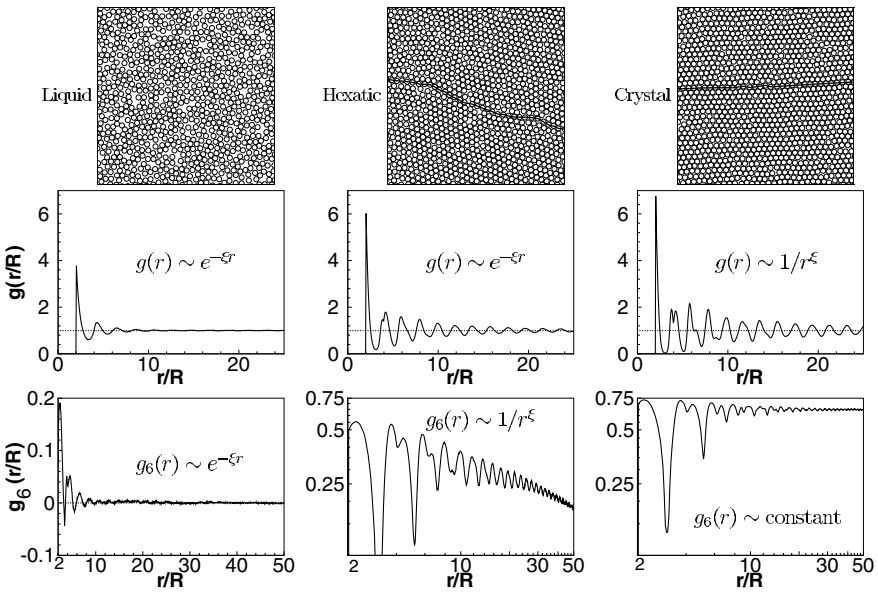

FIG. 2. Temporal evolution of KTHNY phase behavior by direct observation, pair distribution function $g(r)$, and orientational distribution function $g_6(r)$ for tether length $L/R = 5$. Left to right: $\gamma a/A = 35.1$, 1.66×10^4, and 1.70×10^5; $\theta = 0.565$, 0.707, and 0.744.

(straight line in Fig. 2), quasi-long-range translational order $[g(r) \sim 1/r^{\xi}]$ and true long-range orientational order $[g_6(r) \sim \text{const}]$. Phase determination for systems at a given time is determined by plotting $g_6(r)$ on semilog and logarithmic scales and visually evaluating the linearity of the function decay. Within the resolution of the finite box size and the oscillations of the $g_6(r)$ function, a decay indicating hexatic order can be distinguished above a slope of roughly 0.02.

Figure 3 shows the phases observed in the simulations for a variety of tether lengths. The phases are shown as a function of simulation time and as a function of surface coverage. For tether lengths $L/R < 1.25$, only liquidlike order is observed. Hexatic order is observed at higher coverages for $1.25 \leq L/R \leq 3.75$, except for the case of $L/R = 1.5$, where only liquid structure is observed. Systems with $L/R \geq 4$ develop from the liquid through the hexatic and finally to the crystalline phase. In general, the transition to the hexatic phase occurs near $\theta = 0.70$, and the hexatic to crystal transition occurs near $\theta = 0.735$. Systems with $L/R < 4$, which do not crystallize, have coverages as high as $\theta = 0.765$, well above the hexatic to crystal transition point at longer tether lengths. Thus, the tether — or the restricted local mobility — frustrates the phase transition, and the lack of a phase change is not due to low disk density. The tether length versus time phase diagram shows more dramatically how the tethers frustrate ordering. Relative to those that order, systems that are frustrated by short tether lengths can undergo an order of magnitude of time of more diffusion and still not experience a phase change.

No theoretical derivation exists for RSA systems with a locally restricted amount of surface diffusion, a case which represents a straightforward bridge between a completely kinetic system and an equilibrium system. For the case of infinite tether length (i.e., free diffusion on the surface), the power law kinetic extrapolation in Fig. 1 gives the jamming limit of $\theta_\infty = 0.85$ which is less than the close-packed areal fraction of disks in a plane ($\theta_{\text{cp}} = 0.9069$) expected by some [9]. A perfectly packed surface exhibits both long-ranged orientational and translational orders. However, a two-dimensional system is unable to dissipate long wavelength thermal fluctuations, prohibiting long-range translational order. Therefore, it is the thermal fluctuations in the present system that most likely prevent the RSA process from achieving a close-packed configuration. If this hypothesis is correct, this is an unusual manifestation of the symmetry restrictions of two-dimensional space in that it arises in a dynamical process.

The existence of an equilibrium hexatic phase and the order of the transition(s) in two dimensions is currently under debate [10,11]. If a hexatic phase does not in fact exist in an equilibrium system, then the transitions observed in our simulation are significant because they *only* occur in a nonequilibrium process. If the hexatic phase does exist in equilibrium, then our results demonstrate the ability

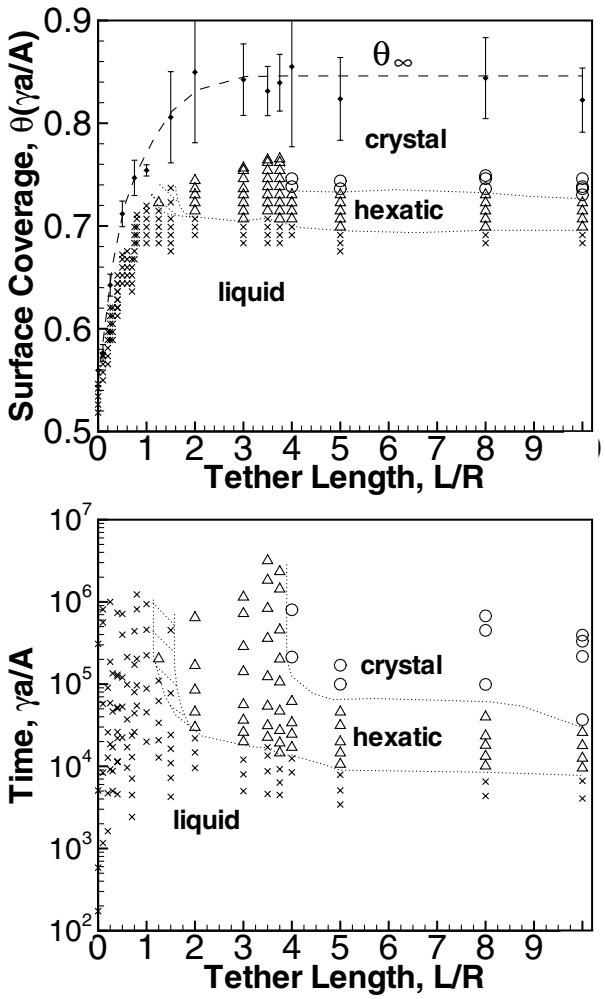

FIG. 3. Phase diagrams of tether length versus coverage (top) and tether length versus time (bottom). Filled points and error bars in the top figure represent jamming limit extrapolations according to Eq. (1).

to control the phase behavior based on the length of the tethers.

KTHNY-style phase transitions occur in the nonequilibrium RSA system when adsorbed disks have sufficient local entropic freedom. In hard sphere systems, crystallization has been interpreted as a sacrifice of global entropy of liquidlike disorder for the local entropy of individual spheres within their lattice "cages." Here, the local freedom of each individual particle can be tuned to either allow or prevent the global restructuring necessary to complete a phase change. Surprisingly, the liquid-hexatic phase boundary between $1 \leq L/R \leq 2$ reveals that particles need to move only slightly more than one particle radius to allow hexatic ordering.

There are several caveats to note in this study, including the finite time of the simulations, finite box-size effects, and the effect of varying diffusion time. In the tether length versus coverage phase diagram, there is a significant separation between the maximum final coverage in the simulation and the θ_∞ boundary. It is fair to wonder if hexatically

ordered structures will become crystalline given enough simulation time and additional coverage. The tether length versus time phase diagram, however, reveals phase boundaries that are more tempting to extrapolate. Since the phase boundaries extend vertically over an order of magnitude of time, one may infer that the boundaries may persist indefinitely at the given tether lengths. It may, in fact, be possible to access more of the phase diagram using experimental nanoparticle systems with covalent tethers. A scaling analysis for 20 nm diameter particles deposited from a 1% aqueous suspension in a simulation of $N_{\mathrm{att}} = 10^6$ adsorption attempts per equivalent particle area shows that the simulated time is

$$t \sim \frac{N_{\mathrm{att}}}{\phi k_{\mathrm{att}}} \sim \frac{N_{\mathrm{att}}\sigma^2}{\phi D} \sim \frac{N_{\mathrm{att}}\sigma^2 3\pi\eta\sigma}{\phi kT} \sim \frac{(10^6)\,(20\ \mathrm{nm})^2(3\pi)\,(1\ \mathrm{cP})\,(20\ \mathrm{nm})}{(0.01)\,(1.381\times 10^{-23}\ \mathrm{J/K})\,(298\ \mathrm{K})} \sim 2000\ \mathrm{s}, \tag{2}$$

where k_{att} is the rate constant for adsorption attempts per equivalent particle area, σ is the diameter of the particles, ϕ is the volume fraction of the depositing suspension, D is the diffusivity of the particles, η is the viscosity of the liquid, k is Boltzmann's constant, and T is temperature. Given this accessible amount of time, it is foreseeable that these predictions could be verified in experimental systems of nanoparticles.

The reported phase boundaries and kinetics hold quantitatively when doubling or halving the simulation box length. However, for the largest boxes tested ($200R \times 200R$), some hexatic phases appeared to exhibit a degree of polycrystallinity. These results are not discussed here because more extensive testing is necessary to capture the polycrystalline phase behavior of large systems.

Changing the amount of diffusion time in the simulations quantitatively affects the phase boundaries. As the number of diffusion steps per adsorption attempt is increased, the systems achieve the hexatic phase and crystalline phases both sooner and for slightly lower tether lengths. For example, when the diffusion is halved, the critical tether length necessary to achieve hexagonal ordering increases from $1.25R$ to $1.5R$, and when the diffusion is doubled, the critical tether length to achieve crystalline ordering decreases from $4R$ to $3.75R$. Although these shifts are not large, they emphasize the *nonequilibrium* nature of the system arising from the irreversible placement of particle anchors. Phase changes reported here are *process dependent*.

In summary, we have studied the kinetic and structural phase behavior of the model nonequilibrium process of assembling a monolayer of disks with locally restricted surface diffusion. We observe a liquid-hexatic-crystal transition that follows the KTHNY scheme. Transitions from liquid to hexatic occur for $L/R > 1$, and $L/R \geq 4$ is necessary for crystal formation. This study provides timely insight into the assembly of nanoparticle systems, which require careful attention to the formation process of superlattice assemblies for use in new applications such as quantum dot array sensors and memory devices.

*Electronic address: jeff@che.utexas.edu
†Corresponding author.
Electronic address: rtb@che.utexas.edu
‡Corresponding author.
Electronic address: korgel@che.utexas.edu

[1] J. M. Kosterlitz and D. J. Thouless, J. Phys. C **6**, 1181 (1973).
[2] B. I. Halperin and D. R. Nelson, Phys. Rev. Lett. **41**, 121 (1978).
[3] A. P. Young, Phys. Rev. B **19**, 1855 (1979).
[4] J. Feder, J. Theor. Biol. **87**, 237 (1980).
[5] M. P. Allen and D. J. Tildesley, *Computer Simulation of Liquids* (Oxford University Press, Oxford, 1987).
[6] R. H. Swendsen, Phys. Rev. A **24**, 504 (1981).
[7] J.-S. Wang and R. B. Pandey, Phys. Rev. Lett. **77**, 1773 (1996).
[8] *Bond Orientational Order in Condensed Matter Systems,* edited by K. J. Strandburg (Springer-Verlag, New York, 1992).
[9] G. Tarjus, P. Schaaf, and J. Talbot, J. Chem. Phys. **93**, 8352 (1990).
[10] A. Jaster, Phys. Rev. E **59**, 2594 (1999).
[11] H. Weber, D. Marx, and K. Binder, Phys. Rev. B **51**, 14 636 (1995).